#### **Bachelor Thesis**

# Decomposing N-Dimensional Unitaries into Local Gates for Quantum Simulation

Alexander Roth

FACULTY OF PHYSICS

May 28, 2025

Supervisors:

Dr. Philipp Preiss

Dr. Titus Franz

## Bachelorarbeit

# Lorem Ipsum

Alexander Roth

FAKULTÄT FÜR PHYSIK

May 28, 2025

Supervisors:

Dr. Philipp Preiss

Dr. Titus Franz

# Contents

# List of Figures

# List of Tables

## Introduction

The simulation of quantum mechanical systems presents a formidable challenge for classical computers. Representing the state of an n-particle quantum system requires tracking  $2^N$  complex amplitudes, leading to an exponential explosion in both memory requirements and computational time as N grows. Consequently, accurately simulating phenomena such as high-temperature superconductivity, the intricate reaction pathways of large molecules in quantum chemistry, or other strongly correlated many-body systems quickly becomes infeasible, even on the most powerful supercomputers. In 1982, Richard Feynman envisioned a groundbreaking solution: a computer built from quantum mechanical elements could effectively simulate these complex quantum problems [?]. Modern quantum computers aim to realize this vision by implementing arbitrary unitary operators on a system of qubits. While significant progress has been made, current quantum computers are still limited in scale and often struggle to outperform classical computers using tensor networks for many relevant problems [?].

As a powerful near-term alternative, (analogue) quantum simulators have emerged. These devices are designed to directly implement a specific target Hamiltonian, leveraging the inherent quantum nature of their constituents such as entanglement and many-particle behavior to explore complex physical phenomena. Quantum simulators can be build using different architectures - ranging from trapped ions, quantum dots, superconducting circuits to ultracold neutral atoms [?]. Ultracold neutral atoms trapped in optical lattices have proven to be a particularly versatile and promising platform for quantum simulation. They provide a high degree of controllability, allowing single-atom and single-site resolution to measure (non-local) correlation functions and counting statistics via quantum gas microscopes [?, ?].

A compelling direction in this field is the convergence of gate-based quantum computation and quantum simulation. The FermiQP project, for example, aims to develop a quantum processor based on ultracold fermionic Lithium (<sup>6</sup>Li) operable in two distinct modes: an analogue mode for quantum gas microscopy and simulation of quantum materials, and a digital mode for quantum computation. The goal of such platforms is to combine the

strengths of both approaches leveraging analogue simulation capabilities while introducing the programmability of gate-based operations.

Nevertheless, the system restricts operations to single- or two-qubit gates, limiting atom manipulations to individual or adjacent lattice sites. Only recently, [?] demonstrated complete access to arbitrary states on the Bloch sphere using nearest-neighbor (NN) gates, enabling the preparation of any desired initial state. However, if precise control over these local interactions is possible, the central question becomes: how can we systematically combine them to achieve any desired global N-atom unitary?

This thesis investigates algorithms to systematically construct arbitrary N-dimensional unitary operations using sequences of these experimentally accessible local gates. It will explore the application of this decomposition to implement crucial quantum operations such as

- Atom Rearrangement (Permutation Matrices): Essential for preparing arbitrary initial Fock states, correcting defects in atom loading, and all-to-all connectivity in the simulator
- Discrete (Fractional) Fourier Transformations: Necessary for transitioning between position and momentum space representations, measuring momentum distributions, probing kinetic energy terms, and implementing protocols for entanglement measurement or quantum phase estimation.

Furthermore, the impact of realistic experimental noise on the fidelity of these decomposed operations will be analyzed and the extension of these one-dimensional decomposition concepts to two-dimensional lattice structures discussed.

#### 1.1 Fermi-Hubbard Model

The Fermi-Hubbard Model is a simplified model which is often used to describe fermions in a solid and is based on the tight binding model. Its Hamiltonian considers a one-particle contribution, which describes hopping, and a two-particle on-site interaction which is the shortest possible. Although the Hubbard model can be viewed as the simplest model of correlated electrons, it is still describing many interesting phenomena in nature like magnetic ordering, metal-insulator transition, or (high-temperature) superconductivity. Therefore, the Hubbard model is the basis for researchers interested in these properties. Its Hamiltonian is given by

$$\hat{H}_{hub} = \hat{H}_{kin} + \hat{H}_{int} = \sum_{x,y \in V,\sigma} t_{xy} c_{x,\sigma}^{\dagger} c_{y,\sigma} + \sum_{x} U_{x} c_{x\uparrow}^{\dagger} c_{x\downarrow}^{\dagger} c_{x\downarrow} c_{x\uparrow}$$
(1.1)

where x and y are spatial directions,  $c_i^{\dagger}$  and  $c_i$  are the fermionic creation and annihilation operators, V is the vertex set,  $t_{xy}$  is the hopping amplitude between sites x and y and

 $U_x$  is the on-site interaction, often the Coulomb interaction. For a lattice, one usually only considers nearest-neighbor hopping, meaning that  $t_{xy} = t$  for |x - y| = 1 and t=0 otherwise [?].

## Theoretical Background

#### 2.1 Quantum Information

#### 2.2 Trapping on a Lattice

To simulate Hubbard dynamics, the FermiQP experiment traps ultracold fermions in an optical lattice. An optical lattice is created by a standing laser light which acts as a periodic potential due to the Stark shift. The FermiQP supperlattice structure is created by two superimposed lattices, creating double wells, allowing for four fermionic modes, two spin modes on two sites  $(|L,\uparrow\rangle,|L,\downarrow\rangle,|R,\uparrow\rangle,|R,\downarrow\rangle)$ . In this thesis, only the noninteracting case is being considered. This reduces the amount of fermionic modes to two  $(|L\rangle,|R\rangle)$ .

#### 2.3 Motional Gates

To run quantum algorithms on a lattice, one needs to perform gates on it. Experimentally, not all gates are equally easy to implement.

Some of the most fundamental gates are the Pauli matrices

$$\hat{X} = \begin{pmatrix} 0 & 1 \\ 1 & 0 \end{pmatrix} \; ; \; \hat{Y} = \begin{pmatrix} 0 & -i \\ i & 0 \end{pmatrix} \; ; \; \hat{Z} = \begin{pmatrix} 1 & 0 \\ 0 & -1 \end{pmatrix} \tag{2.1}$$

and Pauli-Rotation Gates:

$$\widehat{X}(\theta) = e^{-i\frac{\theta}{2}\widehat{X}} \; ; \; \widehat{Y}(\theta) = e^{-i\frac{\theta}{2}\widehat{Y}} \; ; \; \widehat{Z}(\theta) = e^{-i\frac{\theta}{2}\widehat{Z}}$$
 (2.2)

Especially important for us is the  $\widehat{X}(\frac{\pi}{2})$  rotation gate which is a real tunneling operation (see also Figure ??). This also corresponds to a 50:50 beam splitter in optics. The matrix

Figure 2.1: The  $\widehat{X}(\frac{\pi}{2})$  gate applied on the initial state (a)  $|0\rangle$  and (b)  $|1\rangle$  shown on the Bloch-sphere.

Figure 2.2: On a lattice, a the  $\widehat{X}(\pi/2)$  matrix corresponds to real tunneling in the double well and the  $\widehat{Z}(\theta)$  matrix can be implemented by a chemical potential, tilting one of the potential wells.

representation of the operator looks like

$$\widehat{X}(\frac{\pi}{2}) = \frac{1}{\sqrt{2}} \begin{pmatrix} 1 & i \\ i & 1 \end{pmatrix}. \tag{2.3}$$

Figure ?? shows how this gate acts on the two modes of a site, if in the site sits no fermion, we label it  $|0\rangle$ , otherwise if there is a fermion, we label it with  $|1\rangle$ .

The  $\widehat{Z}(\theta)$  can be implemented in the lattice through using the chemical potential (see Figure ??). The optics analogy would be a phase shifter.

As a last gate, we want to take a look at the SWAP operator. This gate simply swaps the two lattice sites, so the effect on an atom in the double well is

$$\widehat{SWAP} = \begin{pmatrix} 0 & 1 \\ 1 & 0 \end{pmatrix} \Longrightarrow \widehat{SWAP} |L\rangle = |R\rangle \; ; \; \widehat{SWAP} |R\rangle = |L\rangle \tag{2.4}$$

#### 2.4 Fidelity of Quantum Gates

An important criteria for benchmarking the implementation of a circuit on a quantum simulator is the fidelity. The fidelity gives the probability, how well the desired state can be implemented using the circuit. The fidelity of two quantum states  $|psi_{\rho}\rangle$  and  $|psi_{\sigma}\rangle$  is defined as

$$\mathcal{F} = \left(tr\sqrt{\sqrt{\rho}\sigma\sqrt{\rho}}\right)^2 \tag{2.5}$$

Figure 2.3: The symmetric  $\widehat{Z}$  gate has a periodicity of  $4\pi$  whereas the asymmetric  $\widehat{Z}$  gate has a periodicity of  $2\pi$ 

Figure 2.4: MZI representation with one phase shifter (asymmetric MZI)

Figure 2.5: (a) Reck's scheme is based on a triangle. The optical depth is 2N-3 (in this example 7 which can be seen by following the longest possible path). Every blue rectangle represents a MZI with one phase shifter before and one after it. (b) The Clements scheme is based on a bricklayer structure providing the optimal optical depth of N with the same number of N(N-1)/2 MZI.

where tr is the trace operator and  $\rho$  and  $\sigma$  are the density matrices of the two states. For pure states, this reduces to

$$\mathcal{F} = |\langle \psi_{\rho} | \psi_{\sigma} \rangle|^2 \equiv |\langle \psi_{ideal} | \psi_{obs} \rangle|^2. \tag{2.6}$$

#### 2.5 Interferometry

The solution on how to implement a random unitary matrix through simpler pieces has long been solved in quantum optics.

In 1994, Reck et al. have shown that any  $N \times N$  Unitary matrix can be implemented using only 50:50 beam splitters and phase shifters. The main idea is that the U(N) matrix can be factorized into many two-dimensional beam splitters. These beam splitters are implemented using a mesh of Mach-Zehnder interferometers (MZI). These consist of two 50:50 beam splitters and, depending on the convention, one or two phase shifters (see figure ??). We will use the convention with only one phase shifter, as it is displayed in figure ??, in the following.

#### 2.5.1 Reck and Clements Scheme

In 1994, Reck and Zeilinger showed for the first time, that any Unitary can be realised by a mesh of beam splitters. The Reck decomposition method, implements any unitary through a triangular mesh of beam splitters (see figure ?? (a)). It uses the minimal number of beam splitters but the optical depth is 2N - 3 [?]. Recks scheme can be used for universal multiport interferometers which are used in many areas such as Boson sampling [?], discrete-time quantum walks [?] or as a universal mode analyzer, allowing measurements in any basis [?].

2016, Clements published a paper that improved on Reck's scheme. The Clements scheme uses a rectangular matrix decomposition, which uses the same minimal number of beam splitters, but is more symmetric and also provides the minimal optical depth of N (figure ?? (b)) [?]. Therefore, this decomposition method is much more scalable and even applicable for quantum simulation purposes.

#### 2.5.2 A Note on Conventions

The real Givens rotation matrix can also be seen as a Mach-Zehnder Interferometer (MZI) or a variable beam splitter with a phase shifter in front of the MZI. A MZI consists of two 50:50 beam splitters and a phase shifter in one of the two arms. A basic layout can be seen in figure ??.

This can be described by the following matrix:

$$MZI = \begin{pmatrix} \cos(\theta) & \sin(\theta) \\ \sin(\theta) & \cos(\theta) \end{pmatrix}$$
 (2.7)

The 50:50 beam splitter matrix is not unique, equation ?? is one possibility and the one we are going to use. But one might also use the below matrices:

$$\frac{1}{\sqrt{2}} \begin{pmatrix} 1 & 1 \\ 1 & -1 \end{pmatrix} \quad or \quad \frac{1}{\sqrt{2}} \begin{pmatrix} -1 & 1 \\ 1 & 1 \end{pmatrix} \tag{2.8}$$

To get to the imaginary givens matrix in equation ??, we have to add another phase shifter after every MZI. This also agrees with the theorem, that every 2x2 matrix can be represented by using three Pauli rotation matrices with free parameters. [?] is using a different convention for the beamsplitter, already incorporating the last phase shifter in the variable Beamsplitter:

$$T_{m,n}(\theta,\phi) = BS(\theta,0)PS(\phi) \tag{2.9}$$

We will not use the Clements notation and stick to the longer form.

Since the 50:50 beam splitter can be represented by a  $\widehat{X}(\frac{\pi}{2})$  gate and a phase shifter by a  $\widehat{Z}(\theta)$  gate, we arrive at the gate sequence

$$T_{m,n}(\alpha,\beta) = \widehat{Z}(\theta)\widehat{X}(\frac{\pi}{2})\widehat{Z}(\phi)\widehat{X}(\frac{\pi}{2})\widehat{Z}(\psi)$$
 (2.10)

which we will call in the following Z3X2.

## Algorithm

#### 3.1 Decomposing a N-dimensional Unitary

Mathematically, both the Reck and the Clements scheme decompose the U(N) matrix using U(2) matrices acting on a 2-dimensional subspace of the Hilbert space [?]. These U(2) matrices can be implemented in the optical setup by using two 50:50 beam splitters and three phase shifters acting on wires n, m that can be represented by the following matrix:

The matrix  $T_{n,m}(\theta,\phi)$  resembles a Givens rotation. A Givens rotation is a rotation in a plane and, if applied from the right, mixes two columns in the same row. It is often used to null specific elements of a matrix in numerical methods. Both schemes follow the QR decomposition algorithm, with which one can find a decomposition of U into an upper triangular matrix (R) and a number of Givens rotations (Q):

$$U(N) = Q * R \tag{3.2}$$

Since U is unitary, R is not only an upper diagonal matrix but has to be a diagonal matrix with modulus 1 and complex entries which we will call D in the following. This is because Q is by design unitary and the since U is unitary, the product is unitary. The only unitary

Figure 3.1: The Clements decomposition starts by nulling the bottom left matrix entry by multiplying a givens rotation from the right. Then, one nulls the adjacent subdiagonal by multiplying givens rotations from the left. One continues in this snake-like pattern until all elements below the diagonal are 0. By finding a matrix D' and reordering the givens decomposition we find the desired structure of eq??.

Figure 3.2: (a) The Clements Scheme creates a brick layer structure which allows for optimal circuit depth of N - in this example N=8. The phase matrix at the end is not necessary since we are measuring right after but is still shown for the sake of completeness. (b) We can further decompose each rotation block into  $\widehat{X}$  and  $\widehat{Z}$  gates which correspond to real tunneling and chemical potential, respectively, when implementing on a lattice. (c) The angles for a discrete Fourier Transformation do not differ in the first layer of the  $\widehat{Z}$  gates (so  $\beta$  is constant. This would even allow to implement all first  $\widehat{Z}$  gates globally, which would improve the overall fidelity.

upper triangular matrix is a diagonal matrix.

To decompose U into Q and R, one has to multiply givens rotations from both left and right. The order in which the Givens rotations are applied is not arbitrary. One starts from the bottom-left corner and moves to the nearest subdiagonal, moving from top to bottom [?]. This is also illustrated in figure ??.

The decomposition of an arbitrary Unitary of dimension N in a diagonal matrix and Givens Rotations is therefore:

$$U(N) = D\left(\prod_{(m,n)\in S} T_{m,n}\right) ; n, m \in [0, N-1]$$
(3.3)

where S is the specific ordered sequence of givens decompositions [?].

To implement the decomposition of a unitary U(N) into Givens decompositions in PennyLane, the givens\_decomposition function from the PennyLane Python library, v.0.40.0, can be used to create the decomposition of an arbitrary input unitary into the form of equation ??. Since in interferometry beam splitters and phase shifters are used to create the Givens rotations, which can be seen as  $\widehat{X}(\pi/2)$  and  $\widehat{Z}(\theta)$  gates, respectively, we can further decompose any of the  $2 \times 2$  Givens rotations into three  $\widehat{Z}$  and two  $\widehat{X}(\pi/2)$  gates as described in eq ??. Figure ?? (a) and (b) illustrate the two steps in this decomposition. The code for the decomposition of the single Givens rotations into Z3X2 can be seen in Appendix ??.

It is important to note, that all calculations are in the non-interacting case. Therefore, we can limit ourselves to the N-dimensional non-interacting subspace of the  $2^N \times 2^N$  total Hilbert space.

#### 3.2 Use Cases

By being able to realise any unitary matrix through local gates opens up numerous opportunities for quantum simulation where one is often hamstringed by the limited gates and therefore operations possible on the lattice.

In this thesis, the focus is on two very important use cases, the first being atom rearrangement and the second a discrete Fourier Transformation.

#### 3.2.1 Rearrangement

Atom rearrangement is of great importance in quantum simulation for different reasons. Firstly, while preparing the lattice for simulations, it needs to be loaded with atoms. Errors can occur and lattice sites might be empty. To ensure that every lattice site contains an atom, one can implement a permutation matrix through the algorithm, which switches atoms from auxiliary lattice sites into the actual simulator.

Secondly, while performing simulations it is necessary to entangle atoms over the whole lattice. Therefore, when simulating, one needs all-to-all connectivity which can be provided with this algorithm. One can again apply whatever permutation matrix is desired to move atoms through all lattice sites. Of course, for this to work in this framework, the interactions U have to be turned off, but turning interactions off and on again is possible, therefore one could move an atom from the bottom left to the top right, turn interaction on and entangle it with its neighbor, turn interaction back off, and move it back.

#### 3.2.2 Discrete (Fractional) Fourier Transformation

The Fourier Transformation and by extension the Fractional Fourier Transformation (which is the more general case) are a necessary tool when simulating on quantum devices. It is necessary for measuring entanglement entropy [?], quantum phase transitions [?] and observables like the static structure factor or excitation spectra [?]. Additionally, kinetic energy terms become diagonal in the momentum space which makes it easier to measure [?].

An example of where one needs to implement a fractional Fourier Transformation (FrFT) are Bell inequality tests. These require to measure between complementary bases (like momentum and position basis). A FrFT can be utilized to measure in both bases [?]. To measure momentum space, a standard method is to switch the optical lattice and harmonic trapping potential off and perform a time-of-flight imaging. This method, though, has a number of limitations. The measuring quality is affected by the inhomogeneity of the trapping potential and the accuracy of the absolute number of atoms is around  $\pm 10\%$  [?]. With the above described algorithm, we are able to implement a discrete Fourier

3.2. Use Cases

Transformation on the lattice. This allows to measure momentum space directly without workarounds and would only be limited by the gate fidelities. Figure ?? shows the example decomposition for a 8 dimensional discrete Fourier transformation including the angles for the  $\widehat{Z}$  gates.

## Error Analysis

#### 4.1 Random Noise on the Gate

#### Multiplicative Noise Model

Figure 4.1: Noise is applied on every Z gate's angle via  $\theta = \theta_0(1 + \sigma)$ . Each system size was 100 runs. The fidelity plotted against the noise is shown for a random unitary. Lines are drawn to improve readability. To reach a Fidelity of better than  $1 - \mathcal{F} = 10^{-3}$ , we need a noise in the range of  $10^{-3}$ 

Figure 4.2: Noise is applied on every Z gate's angle via  $\theta = \theta_0(1 + \sigma)$ . Each system size was 100 runs. The fidelity plotted against the noise is shown for a permutation matrix where the input states were randomly chosen. Lines are drawn to improve readability. To reach a Fidelity of better than  $1 - \mathcal{F} = 10^{-3}$ , we need a noise in the range of  $10^{-3}$ 

#### Additive Noise Model

#### 4.2 Correlated Errors

When applying the  $\widehat{Z}$  gates locally on the lattice, it is possible that a tail of the potential is leaking into the neighboring lattice site. To simulate how concise the beam waist has to be, we are applying a nearest neighbour crosstalk error onto the  $\widehat{Z}$  gates per layer. We are including only nearest neighbors because we model the beam as an exponential, therefore the second order is negligible.

#### 4.3 Focus on the Permutation Matrix

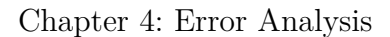
We can consider different cases for the rearrangement. Lets first consider only one atom which is being rearranged in an otherwise empty lattice. Additionally, we are only working

Figure 4.3: (a) The error scales linearly with the system size N. The line is a linear fit to improve readability. The data was taken for an error of  $\sigma = 10^{-3}$ . (b) The matrix decomposition is robust against different input states.

Figure 4.4: Noise is applied on every Z gate's angle via  $\theta = \theta_0 + \sigma$ . The diagrams are for 100 runs each. (a) Fidelity for a random Unitary, (b) for a permutation matrix. Lines are drawn to improve readability. To reach a Fidelity of better than  $1 - \mathcal{F} = 10^{-3}$ , we need a noise in the range of  $10^{-3}$  to  $10^{-2}$ 

with computational basis states. If we are now decomposing the single nearest neighbor  $\widehat{SWAP}$  matrix into the Z3X2 layout, we are finding the angles (0,0,0) for the three  $\widehat{Z}$  gates. Therefore, when applying a multiplicative (or also additive) error to the gate's angle, we are not getting any diagonal elements in our reconstructed  $\widehat{SWAP}$  gate and we will not pick up any error on our  $\widehat{SWAP}$  besides a phase. But we do pick up an off diagonal error for the Identity matrix, the angles in the decomposition are  $(\pi,\pi,0)$ . This does not result in a reduced fidelity in this case since we are only looking at one atom in a lattice and since there are no other atoms which can pick up an error through the identity the fidelity should always be 1.

This in itself is already a pretty interesting result but it gets even more interesting: We now want to consider one swapping atom but also one atom which is only exposed to identity gates (figure (b)). The swapping atom, as discussed, does not pick up an error during the rearrangement process. The other atom, on the other hand, will pick up an error due to the imperfect implementation of the identity matrix. The off-diagonal error is of order  $\mathcal{O}(\varepsilon)$  which can be seen by Taylor-expanding the because of the error non-zero off-diagonal element  $1 - e^{-i\pi\varepsilon}$ . There is also the option to be able to implement the identity perfectly and have the error on the  $\widehat{SWAP}$  gate by switching the second  $\widehat{X}$  gate to  $\widehat{X}(3\pi/2)$ . This can be advantageous, depending on the desired matrix. Another interesting question is what happens if when implementing the identity, there is another Fermion in the second site. Pauli blocking should prevent any interaction???????



14

Figure 4.5: (a) The diagram shows the crosstalk error for a DFT (N=10). The multiplicative noise model has been used and was applied on all  $\hat{Z}$  gates. To get below a Fidelity of  $1 - \mathcal{F} = 10^{-3}$ ,  $\varepsilon < 10^{-3}$ .

Figure 4.6: If the system size increases,  $\varepsilon$  has to decrease as well to still allow to get below the  $10^{-3}$  threshold.

Figure 4.7: (a) With only one atom in the lattice, the fidelity in our error model will always be 1 since we do not pick up any error in the SWAP gate. (b) The swapping atom in site 2 is not picking up any error, the atom in lattice site 3, on the other hand, will pick up an error because of the imperfect implementation of the identity. (c) In this case, any operation on the lattice sites 3 and 4 is not being implemented because of pauli blocking. Therefore, we will not pick up any error by applying the identity so our fidelity will be 1

## Transition to Two Dimensions

Up until this point, we only considered a one dimensional array of atoms. To allow for the general case of applying a matrix (e.g. a two dimensional Fourier Transformation), we need to find a generalisation for two dimensions.

#### 5.1 General Unitary Matrices

Of course one could easily expand the 2 dimensional  $N \times N$  lattice structure into a  $N^2$  array. This means that the rank 4 tensor is expanded into a  $N^2 \times N^2$  matrix [?]. This works for every rank 4 tensor. The problem with this approach is, though, that the depth is of  $\mathcal{O}(N^2)$  which makes it difficult to go to large system sizes as one can see in the Chapter ??. As a short proof one can look at the Clements decomposition which uses  $N^2$  gates for a  $N \times N$  matrix. Therefore, to account for the added information, now  $N^4$  gates are required. Since one can only apply  $N^2/2$  gates simultaneously on the lattice, the shortest circuit (and therefore optical depth) is

$$\mathcal{O}(N^4)/\mathcal{O}(N^2) = \mathcal{O}(N^2).$$

Depending on the system size and error tolerance, this might be a suitable method after all and there is no further thinking required. It is, though, possible to get below  $\mathcal{O}(N^2)$  depth by applying different schemes or using underlying symmetries in the tensors. For both cases that this thesis looks at, this is in fact the case.

#### 5.2 Permutation Matrix

To implement a permutation matrix on an  $N \times N$  lattice, the overall rearrangement must be broken into three sequential passes—rowpermute, columnpermute, then rowpermute again so that the core algorithm is applied three times in total. This threestep decomposition is necessary because each step can only manipulate entire rows or entire columns

Figure 5.1: When rearranging in a lattice, conflicts can occur. (a) we see such a conflict. The atoms at sites (2,1) and (3,1) are supposed to move to (0,4) and ((0,3), respectively. If we first do operations on all rows, we run into a conflict in row 3 since there is an atom occupying site (3,3). If we operate first on all columns we run into the conflict that both moving atoms have to move to the row 0. (b) To resolve these conflict we introduce auxiliary lattice sites in light blue. (c) We can only operate on all rows or columns but not a mix. Therefore, we propose that the atoms move first horizontally to the auxiliary sites, then move to the target rows and finally move with a horizontal permutation to the desired target state. In total, we always need maximum of N auxiliary columns which results in a maximum circuit depth of  $\mathcal{O}(5N)$ .

at once. In case one can target individual double wells arbitrarily, a runtime proportional to the maximal Manhattan distance could be achieved, namely  $\mathcal{O}(2N)$ . The Manhattan distance between two points  $(x_1, y_1)$  and  $(x_2, y_2)$  is

$$|x_1-x_2|+|y_1-y_2|,$$

and on an  $N \times N$  grid the maximum such distance (between opposite corners) is 2(N-1). Since this is not possible in the FermiQP experiment, the HVH scheme is required. The idea is that in the first row-permute, atoms are moved to an auxiliary lattice. In this lattice, atoms are moved to the target row in the column-permute and in the final row-permute back into the main lattice to the target site. This is shown in figure ?? (c). The auxiliary lattice, as well as the three steps, are needed to resolve conflicts as shown in figure ?? (a). To make sure that all conflicts are resolved, the auxilliary lattice needs to be of size NxN. Therefore the row-permutes can be implemented with  $\mathcal{O}(2N)$  and the column-permute can be implemented with  $\mathcal{O}(N)$ . Since both are of order of N and the circuit depth is additive, the final circuit depth is also of  $\mathcal{O}(N)$ .

#### 5.3 Discrete Fourier Transformation

For implementing a DFT there is a much simpler and more straight forward solution to reach a circuit depth of  $\mathcal{O}(N)$ . The idea is to use the separability of the (discrete) Fourier transform, meaning that the 2 dimensional DFT can simply be written as

$$DFT_{N\times N} = DFT_{N,columns}(DFT_{N,rows}).$$

This can be easily seen:

**Theorem 1** (Separability Theorem). Let f be a function on the discrete grid  $\{0, 1, \dots, N-1\}$ 

1}  $\times$  {0, 1, ..., M-1}. Then its two-dimensional discrete Fourier transform

$$DFT(u,v) = \frac{1}{\sqrt{N}} \frac{1}{\sqrt{M}} \sum_{x=0}^{N-1} \sum_{y=0}^{M-1} f(x,y) e^{-j2\pi \left(\frac{ux}{N} + \frac{vy}{M}\right)}$$

can be written as:

$$DFT(u,v) = \frac{1}{\sqrt{N}} \sum_{x=0}^{N-1} \left( \frac{1}{\sqrt{M}} \sum_{y=0}^{M-1} f(x,y) e^{-j2\pi vy/M} \right) e^{-j2\pi ux/N} = DFT_x(DFT_y(f(x,y)))$$

Therefore, the total circuit depth is a composed out of one dimensional DFTs on all rows and after that one dimensional DFTs on all columns, both of  $\mathcal{O}(N)$  which means that the total circuit depth is still of  $\mathcal{O}(N)$ .

# Conclusion and Outlook

# Appendix A

 ${\bf Decomposition\ into\ ZXZXZ}$ 

Hiermit erkläre ich, die vorliegend	e Arbeit selbständig verfasst zu haben und keine
anderen als die in der Arbeit angegeben	en Quellen und Hilfsmittel benutzt zu haben.
München, den 20.6.2025	
	Unterschrift